Modulation of nightside polar patches by substorm activity

Wood, Alan George; Pryse, Sian Eleri; Moen, J.

Published in:
Annales Geophysicae

DOI:
10.5194/angeo-27-3923-2009

Publication date:
2009

Citation for published version (APA):
Wood, A. G., Pryse, S. E., & Moen, J. (2009). Modulation of nightside polar patches by substorm activity. *Annales Geophysicae*, *27*, 3923-3932. https://doi.org/10.5194/angeo-27-3923-2009

Ann. Geophys., 27, 3923–3932, 2009
www.ann-geophys.net/27/3923/2009/

Annales Geophysicae

Modulation of nightside polar patches by substorm activity

A. G. Wood[1], **S. E. Pryse**[1], **and J. Moen**[2]

[1]Institute of Mathematics and Physics, Aberystwyth University, Wales, UK
[2]Department of Physics, University of Oslo, Norway

Received: 5 January 2009 – Revised: 16 July 2009 – Accepted: 17 September 2009 – Published: 13 October 2009

Abstract. Results are presented from a multi-instrument study showing the influence of geomagnetic substorm activity on the spatial distribution of the high-latitude ionospheric plasma. Incoherent scatter radar and radio tomography measurements on 12 December 2001 were used to directly observe the remnants of polar patches in the nightside ionosphere and to investigate their characteristics. The patches occurred under conditions of IMF B_z negative and IMF B_y negative. They were attributed to dayside photoionisation transported by the high-latitude convection pattern across the polar cap and into the nighttime European sector. The patches on the nightside were separated by some 5° latitude during substorm expansion, but this was reduced to some 2° when the activity had subsided. The different patch separations resulted from the expansion and contraction of the high-latitude plasma convection pattern on the nightside in response to the substorm activity. The patches of larger separation occurred in the antisunward cross-polar flow as it entered the nightside sector. Those of smaller separation were also in antisunward flow, but close to the equatorward edge of the convection pattern, in the slower, diverging flow at the Harang discontinuity. A patch repetition time of some 10 to 30 min was estimated depending on the phase of the substorm.

Keywords. Ionosphere (Plasma temperature and density; Polar ionosphere) – Magnetospheric physics (Storms and substorms)

1 Introduction

This case study from 12 December 2001 investigates the influence of geomagnetic substorm activity on the distribution of ionisation patches in the nightside F-region ionosphere. The patches comprise electron density enhancements of at least twice that of the surrounding ionosphere and have horizontal spatial scales of at least a hundred kilometres (Crowley, 1996). They are likely to be produced on the dayside and transported antisunward by the high-latitude convective flow through the polar region and into the night sector. On the nightside they influence the spatial distribution of the high-latitude ionospheric plasma, which in turn may affect transionospheric radio signals that are of concern to propagation applications.

Patches of ionisation in the polar region were first identified using ionospheric sounders and all-sky imagers (Buchau et al., 1983; Weber et al., 1984), but have since been studied by different experimental techniques, including incoherent scatter radar (Weber et al., 1986; Carlson et al., 2002) and radio tomography (Walker et al., 1999). A comprehensive review of early observations is given by Crowley (1996). Polar patches occur predominantly when the interplanetary magnetic field (IMF) has a negative B_z component (McEwen and Harris, 1996) and drift antisunward in the convection pattern at speeds of typically 300–1000 m s^{-1}. Experimental observations mainly support photoionisation from subpolar latitudes on the dayside as the plasma source (Foster, 1984; Buchau et al., 1985; Pryse et al., 2004; Moen et al., 2006, 2008) with the ionisation being drawn poleward in a tongue-of-ionisation (TOI) (Valladares et al., 1994; Sims et al., 2005). However, production by soft particle precipitation may also contribute (Weber et al., 1984). Several mechanisms have been invoked to explain the breakup of a continuous TOI into patches, for example: modulation of plasma densities by precipitation (Walker et al., 1999; Smith et al., 2000), temporal variations in the convection pattern due to changes in IMF orientation (Sojka et al., 1993), expansion and contraction of the high-latitude convection pattern because of pulsed reconnection (Lockwood and Carlson, 1992; Carlson et al., 2006), convection vortices (Schunk et al., 1994), increased plasma recombination in flow channel events (Rodger et al., 1994) and the effect

Correspondence to: A. G. Wood
(alan.wood@aber.ac.uk)

Published by Copernicus Publications on behalf of the European Geosciences Union.

of the thermosphere on plasma production (Carlson et al., 2007). Moen et al. (2006) presented evidence for segmentation of plasma patches at subauroral cusp latitudes in association with pulsed return flow in the postnoon sector. It was suggested that the downward Birkeland current sheet located at the equatorward boundary of the flow disturbance may represent the actual cutting mechanism. Nevertheless a complete understanding of the structuring processes remains to be obtained.

Studies of polar patches have focussed mainly on their production on the dayside, with fewer studies of the features on the nightside. Weber et al. (1986) presented the first observations of polar cap patches in the nightside ionosphere. A modelling study by Bowline et al. (1996) using the Utah State University Time Dependant Ionospheric Model (TDIM) predicted that the TOI should be a prominent evening feature above Ny-Ålesund in the European sector under conditions of IMF B_z and B_y negative. A comparison of the Coupled Thermosphere-Ionosphere-Plasmasphere (CTIP) model and experimental observations by radio tomography showed the role of the TOI in forming the poleward wall of the mid-latitude trough in the postmidnight European sector (Middleton et al., 2008; Pryse et al., 2009). Polar patches have also been observed in the nightside ionosphere under conditions of IMF B_z positive (Wood et al., 2008).

Boundary blobs are plasma density enhancements which occur in the auroral oval at the equatorward edge of the high-latitude convection pattern (Crowley, 1996). Latitudinally localised soft particle precipitation was suggested as the source mechanism (Rino et al., 1983) whilst modelling predicted that a polar cap patch could exit the polar cap and reconfigure to form a boundary blob (Robinson et al., 1985). Patches have been observed leaving the polar cap (Pedersen et al., 2000; Moen et al., 2007; Lorentzen et al., 2004) and experimental evidence for the reconfiguration of a polar patch into an evening-time boundary blob has been presented (Pryse et al., 2006).

Of particular relevance to this current investigation is the nightside study of Lorentzen et al. (2004), where airglow measured by ground-based photometers was used as a proxy for polar cap patches drifting equatorward from the polar cap into the evening/nighttime sector. The altitude, meridional speed, horizontal extent and repetition interval of the airglow patches were determined using observations from two meridian scanning photometers (MSP) at Longyearbyen and Ny-Ålesund, both on Svalbard, and these were related to the substorm phases. The current investigation complements this earlier study, but here direct observations of the electron density enhancements are presented. These were obtained by the EISCAT (European Incoherent SCATter) Svalbard radar (ESR) and the ionospheric radio tomography experiment of Aberystwyth University located in northern Scandinavia. Variations in the plasma drift were measured by the Super Dual Auroral Radar Network (SuperDARN), while variations in the open-closed field line boundary (OCB) were inferred from both ESR and SuperDARN observations. These were taken collectively to interpret the density modulation. The observations were made on the evening of 12 December 2001 in the antisunward flow near the Harang discontinuity. Geomagnetic conditions were moderately disturbed with K_p=3 between 18:00 UT and 24:00 UT. The Advanced Composition Explorer (ACE) spacecraft, in the solar wind upstream from the Earth, monitored a stable interplanetary magnetic field between 17:00 UT and 23:00 UT, with the exception of a small discontinuity near 19:30 UT. The B_z component of the IMF was ~-5 to ~-6 nT throughout and IMF B_y was ~-2 nT prior to 19:30 UT and ~-4 nT subsequently. Under these pertinent stable conditions, dayside reconnection was unlikely to result in significant modulations of the high-latitude convection pattern.

2 Results

2.1 Magnetic field

Figure 1 shows the horizontal component of the geomagnetic field measured at Tromsø (69.7° N, 18.9° E; 66.6° MLAT, 103.1° MLON) between 18:00 UT and 24:00 UT on the evening of 12 December 2001 by the magnetometer of the Tromsø Geophysical Observatory, University of Tromsø, Norway. Two clear negative deflection bays of ∼350 nT and ∼375 nT are apparent with the minima at 20:18 UT and 22:41 UT respectively, indicating two substorms separated by just over two hours. The declination angle (not shown) was between 3° and 4° throughout this interval, indicating that the overhead current was almost purely zonal. Magnetometer observations to the north and south of Tromsø (not shown) indicated that this disturbance was centred within ∼2° MLAT of Tromsø. As in the study of Lorentzen et al. (2004) these negative deflections are taken as ground signatures of the diverted magnetospheric tail current closing in the ionosphere as the westward electrojet, and an indicator of enhanced nightside reconnection.

2.2 High-latitude electric potential patterns

Plasma drift velocities at northern high-latitudes were measured by the Super Dual Auroral Radar Network (SuperDARN) (Greenwald et al., 1995; Chisham et al., 2007). Measurements made using radars in the Northern Hemisphere may be taken collectively and inverted using the spherical harmonic fitting technique described by Ruohoniemi and Baker (1998) to produce global maps of the high-latitude electric potential. The maps were obtained at 2-min intervals for the duration of the time of interest between 18:00 UT and 24:00 UT, with those at 20 min intervals shown in the panels of Fig. 2. In the summary panels of this figure magnetic noon is at the top of each panel and magnetic latitude is indicated by the grey dashed circular lines in 10.0° increments with 60.0° MLAT at the outer circumference. These panels reveal

the temporal trends apparent in the more frequent plots of the complete data set. Also shown on each panel are the horizontal velocity vectors derived from the ionospheric backscatter measured by the radars that were used to shape the potential patterns. In the ionospheric F-region the $\boldsymbol{E}\times\boldsymbol{B}$ drift transports plasma along the equipotential contours, so that for the duration of the time of interest there are clear indications of a general antisunward flow across the polar cap, and return sunward flows at lower latitudes on the dawn and dusk sides of the cells. The orange line on each panel indicates the latitudinal coverage of the beam of the 32 m-dish of the EISCAT Svalbard Radar (ESR) in the ionospheric F-region at the relevant times. For the particular programme run on the ESR the radar beam alternated between two closely spaced pointing directions. These are described in more detail in Sect. 2.3, but suffice to say at present that the difference between the two beam directions is insignificant on the scale of the panels in the figure and only a single trace is shown. Comparison of the radar beam location with the electric potential pattern shows that the ESR was observing in the vicinity the Harang discontinuity throughout the time interval of interest, initially observing at an MLT just prior to the flow divergence and then at an MLT just beyond the feature at the end of the interval. The entire radar beam was located in the antisunward flow between 19:00 UT and 24:00 UT. Observations of the SuperDARN radar at Hankasalmi, Finland (59.8° N, 26.5° E; 59.8° MLAT, 105.5° MLON AACGM) were made by its 16 beams (labelled 0 to 15) directed generally northward within a fan-shaped area with beam 0 on the western side. The viewing direction of Beam 6 is indicated on each panel in Fig. 2 by the blue line; this beam having been chosen as it was pointing essentially towards the intersection of the ESR 32 m-dish radar beam with an altitude of 350 km. The SuperDARN beam was also in the vicinity of the Harang discontinuity moving from its pre-magnetic-midnight side to the post-midnight side during the interval under consideration.

The interpretation of the electric potentials in some individual panels of Fig. 2 requires caution because of the limited availability of flow measurements in certain regions with spurious contours produced in some panels such as at the lower latitudes on the evening side at 19:20 UT and 19:40 UT. Nevertheless the observations give a good indication of the location of the equatorward edge of the high-latitude convection on the nightside. Close inspection of the panels reveals that this edge exhibits two equatorward expansions at panels 20:00 UT to 20:40 UT and panels 22:20 UT to 23:00 UT, separated by a retreat of the boundary to higher latitudes between about 21:00 UT and 21:20 UT. It is difficult to give precise times of maximum expansions from these plots due to uncertainties in the fitting of the electric potential and the time resolution of the figure. However, the first is identified with the 20:20 UT panel where the return flow of the dusk cell reaches down to almost 60° MLAT, and the second with the 22:40 UT panel when the return flows are likely to extend to latitudes lower than 60° MLAT. In between these

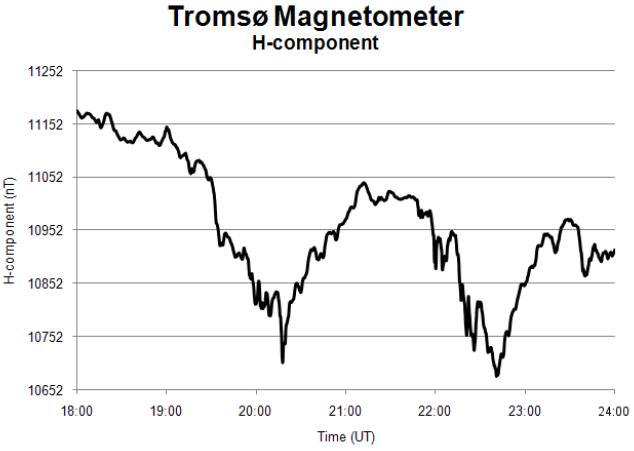

Fig. 1. The horizontal component of the magnetic field observed at Tromsø between 18:00 UT and 24:00 UT on 12 December 2001. The mean value of this component on 12 December 2001, the quiet field, was 11 052 nT.

two extremes, the return flow retreats to poleward of about 65° MLAT. This sequence of two expansions, separated by the contraction, is attributed to the two geomagnetic substorms and is also apparent within the two minute resolution data set (not shown).

2.3 Plasma density and temperature

The 32 m-dish of the EISCAT Svalbard radar (78.2° N, 16.1° E; 75.0° MLAT, 113.1° MLON) observed essentially equatorward at a low elevation of 30° during the experiment, pointing alternatively at azimuths of 170.8° and 185.3° with a dwell time of 64 s at each position. Observations were also made using the ESR 42 m-dish which gave a cycle time of 256 s. However, the measurements from this dish were well outside the region of interest and so are not considered in this paper. Electron densities and temperatures measured by the ESR 32 m-dish between 18:00 UT and 24:00 UT are shown in the panels of Fig. 3 as functions of UT and altitude. The top two panels are for the azimuth of 185.3° and the lower panels for the azimuth of 170.8°. When interpreting the y-axis of these panels, the low elevation of the radar beam should be borne in mind, and that the latitude of the backscatter volume decreases as the altitude increases. For this reason, a geomagnetic latitude scale is inserted on the y-axis. Both electron density panels show clear regions of enhanced densities in the F-region at ionospheric altitudes of between 300 km and 500 km, which correspond to electron temperatures at background levels. The altitude of the peak electron density is 350 km. The altitude and electron temperatures of these enhancements are consistent with those of polar patches that would have convected across the polar cap. The high-altitudes indicate long-lived plasma as the ionisation recombination rate is reduced at these altitudes and the

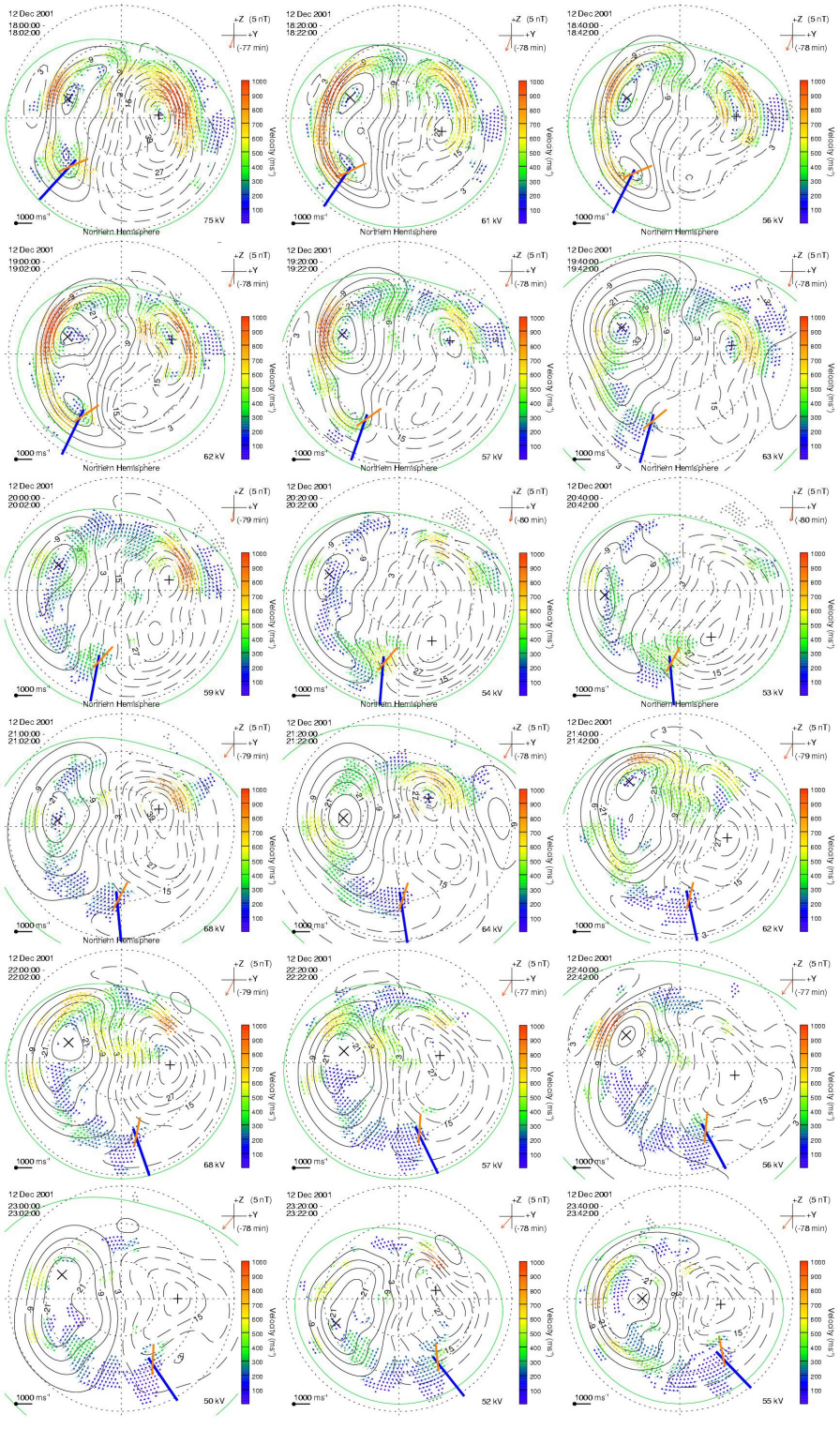

Fig. 2. SuperDARN electric potential patterns at 20 min intervals between 18:00 UT and 23:40 UT on 12 December 2001 as a function of geomagnetic latitude and magnetic local time. Magnetic noon is at the top of each panel with dusk and dawn on the left- and right-hand sides respectively. Magnetic latitude is indicated by the grey dashed circular lines in 10.0° increments with 60.0° MLAT at the outer circumference and the magnetic pole at the centre of each panel. The orange line on each panel indicates the intersection of the 32 m-dish ESR beam observing at an azimuth of 185.3° and elevation 30.0°. The northern extreme of the line is at ground level, and the equatorward extreme is at an altitude of 600 km. The blue line indicates the intersection of beam 6 of the SuperDARN radar at Hankasalmi, Finland.

low electron temperatures rule out in situ plasma production by soft particle precipitation. Several regimes can be identified in the density structure, which are consistently seen by the radar at both pointing directions. Of particular interest are: a region of separate, distinct enhancements from about 19:55 UT to 21:15 UT, an apparently more continuous enhancement between about 21:15 UT and 22:15 UT, a subsequent second region of less intense, but separate enhancements prior to 23:05 UT and another region of an apparently continuous enhancement between about 23:15 UT and midnight. The slanted appearance of enhancements, in particular those in the first interval starting at 19:55 UT, indicate that an enhancement is observed at higher altitude with increasing time. This is due to the observing geometry and direction of the convective flow, which cause the intersection altitude of the radar with an enhancement to increase as a feature moves equatorward away from the radar, rather than an increase in the altitude of the enhancement. Electron temperatures are at background levels during the interval of main interest after about 19:55 UT, with the exception of two regions of significantly higher levels at the highest altitudes (lowest latitudes) around 20:15–20:55 UT and 22:25–22:45 UT. These are discussed in Sect. 2.4.1 but for now it suffices to say that these do not correspond to the enhancements. Equatorward ion drift velocities (not shown) derived from the measurements of the two radar beams are consistent with the equatorward plasma drift observed by the SuperDARN radars near the Harang discontinuity. The greatest velocities of about 400 m s^{-1} are observed in the recovery phase of substorms with lower velocities of about 300 m s^{-1} observed between the substorms.

2.4 Open-closed magnetic field boundary

2.4.1 Electron temperature

Electron temperatures observed by the ESR 32 m-dish and shown in Fig. 3 are at background levels after about 19:55 UT, with the exception of two regions of significantly higher values around 20:15–20:55 UT and 22:25–22:45 UT. The enhanced temperatures at the highest altitudes (lowest latitudes) are signatures of in situ particle precipitation in the auroral region that came into the radar field-of-view during these time intervals due to the poleward expansion of this region. The poleward boundary of the enhanced temperatures can be used to infer the open-closed magnetic field boundary (OCB) (Moen et al., 2004; Østgaard et al., 2005) which separates the open magnetic field lines at higher latitudes from the closed field of lower latitudes. The electron temperature boundary attains the most poleward latitudes of 70° MLAT at 20:25 UT and 71° MLAT at 22:30 UT. These are broadly in agreement with the maxima of the substorms identified from the magnetometer observations.

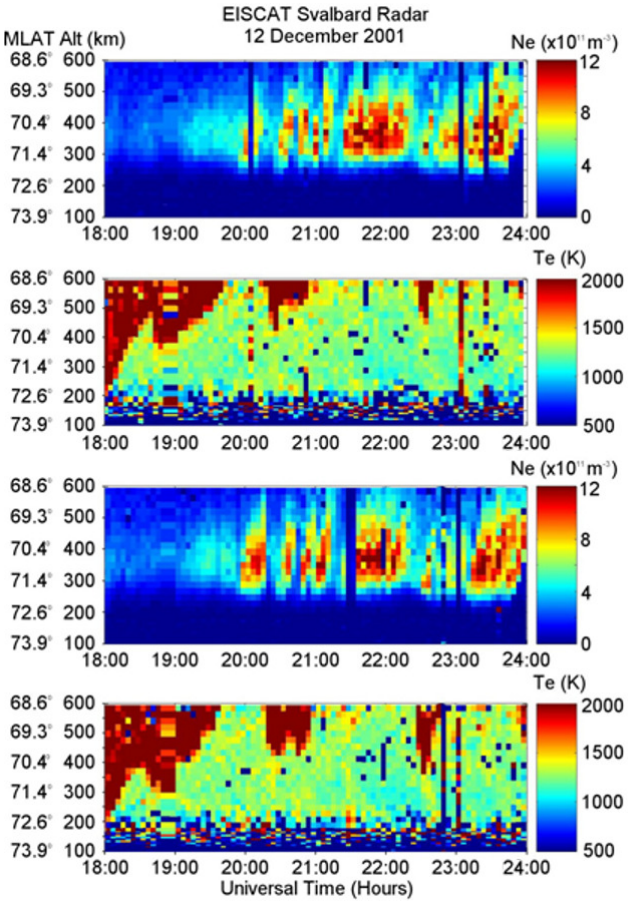

Fig. 3. Electron densities (top panel) and electron temperatures (second panel) measured by the 32 m-dish of the ESR observing at an azimuth of 185.3° and an elevation of 30.0° between 18:00 UT and 24:00 UT on 12 December 2001. Similarly, the electron densities (third panel) and electron temperatures (bottom panel) measured by the ESR observing at an azimuth of 170.8° and elevation of 30.0°.

2.4.2 Spectral width

The spectral width of the line-of-sight velocity measured by each of the SuperDARN radar beams can be used as proxy for the OCB (Chisham et al., 2004). A sharp boundary is often seen between velocities of small spectral width at the lower latitudes and those with a significantly larger spectral width at higher latitudes. A spectral width of 150 m s^{-1} was selected for estimating the transition region in the case of the current observations, with the boundary determined from the measurements of Beam 6 shown in Fig. 4. Threshold values of 100 m s^{-1}, 200 m s^{-1} and 250 m s^{-1} were also considered. These showed the same cycles of expansion and contraction but were displaced in latitude. A threshold value of 150 m s^{-1} was chosen to optimise data coverage. The OCB is 1°–2° poleward of the Spectral Width Boundary (SWB) at this threshold value (Chisham et al., 2004),

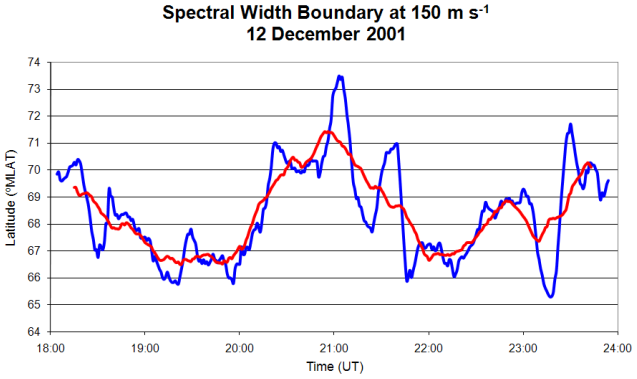

Fig. 4. Spectral Width Boundary (SWB) observed by beam 6 of the Hankasalmi SuperDARN radar between 18:00 UT and 24:00 UT on 12 December 2001. The blue trace represents the SWB smoothed using a 10 min running mean filter, and the red line shows the underlying trend using a 30 min running mean filter.

nevertheless any systematic offset does not alter the validity of this method to infer the motion of the OCB. The blue trace shows the SWB smoothed in time by a 10 min running mean filter, whilst the red curve shows the data smoothed by a 30 min running mean filter. These curves also show a two-cycle pattern with the latitude of the boundary moving to higher latitudes as the auroral region expands poleward during the substorms. In response to the expansion of the first substorm the boundary, which was smoothed by a 30 min running mean filter, starts to move rapidly poleward from a magnetic latitude of about 67° MLAT at about 19:50 UT to some 71° MLAT at 21:00 UT, with the steepest part of the increase between 19:55 UT and 20:30 UT. The latitudinal migration in response to the second substorm occurs at about 22:10 UT with a poleward migration of the boundary from about 67° MLAT to some 69° MLAT prior at about 23:00 UT. In the interval between the substorms, between 21:10 UT and 22:00 UT, the boundary returns to its pre-substorm level, although the 10 min smoothed data shows that there is latitudinal variation on this smaller timescale. The SWB thus also responds to the substorm activity, showing latitudinal variations in response to the two bays in magnetic activity. However, close inspection of the temporal variation in the latitudinal variation in the boundary reveals that there is not a clear one-to-one correspondence between the finer details of the responses. This is a likely consequence of additional variation in the latitude of the SWB on shorter timescales than that of the substorm, apparent in the 10 min smoothed data between 20:50 UT and 21:50 UT.

2.5 Plasma density

The radio tomography experiment of Aberystwyth University measures total electron content along a large number of intersecting transionospheric satellite-to-receiver ray paths. Tomographic inversion of the measurements yields the spatial distribution of the electron density over a latitude-versus-altitude plane (Pryse, 2003, and references therein). Two satellite passes were monitored during the time interval of interest. The tomographic images are shown in the top panels of Fig. 5, where 21:24 UT and 22:19 UT are the times at which the satellites passed over the latitude of 75° N. Both reconstructions show a structured F-region ionosphere with a succession of electron density enhancements in the centre of the field-of-view between about 70° N and 80° N, but with contrasting latitudinal spatial distributions. In the earlier pass the individual enhancements are separated by some 2° latitude, whilst in the later pass the separation between the enhancements is some 5° latitude. Further interpretation of the plasma structuring requires consideration of the observing geometry, the plasma flow pattern and the OCB. The bottom panels of Fig. 5 show the 350 km intersection of the satellite passes superimposed on the SuperDARN electric potential pattern, with the colour code along the trajectory showing the electron density at the F-region peak. Plots from 21:20 UT and 22:18 UT are used to ensure reasonable coverage of backscatter measurements. The SWB as identified from the 30 min running mean of the SuperDARN spectral width measurements is indicated on each panel by a cross, with the OCB located 1°–2° poleward of this location. The trajectories of both passes are seen to lie in the vicinity of the Harang discontinuity. In the earlier pass the enhancements are in the antisunward flow, but only slightly poleward of the OCB near the equatorward edge of a contracted high-latitude electric potential pattern. The electric potential contour equatorward of the OCB is likely to be spurious in the absence of irregularity scatters in this region. By the time of the second pass, the electric potential pattern is expanded to lower latitudes. The two density enhancements, at similar latitudes to those in the earlier reconstruction, now lie well within the main flow of the antisunward plasma drift and are significantly poleward of the OCB. Mention should be made of the difference in the altitude of the density structure in the passes, with that of the earlier pass being some 50 km lower than that of the structure of the later pass. The enhancements seen during the earlier pass are also at lower altitudes than those of the enhancements observed by the ESR. These differences can be attributed to the tomography observing geometry leading to uncertainty in altitude due to lack of measurements along horizontal ray paths. However, this restricted ability of the tomography to determine the altitude of the peak electron density does not detract from the validity of the method to locate the latitudinal locations of the enhancements.

3 Discussion

Central to this study is the spatial structure of the ionospheric F-region plasma in the night sector. The observations focused on ionisation enhancements that had drifted into the region from polar latitudes. Electron temperatures within the

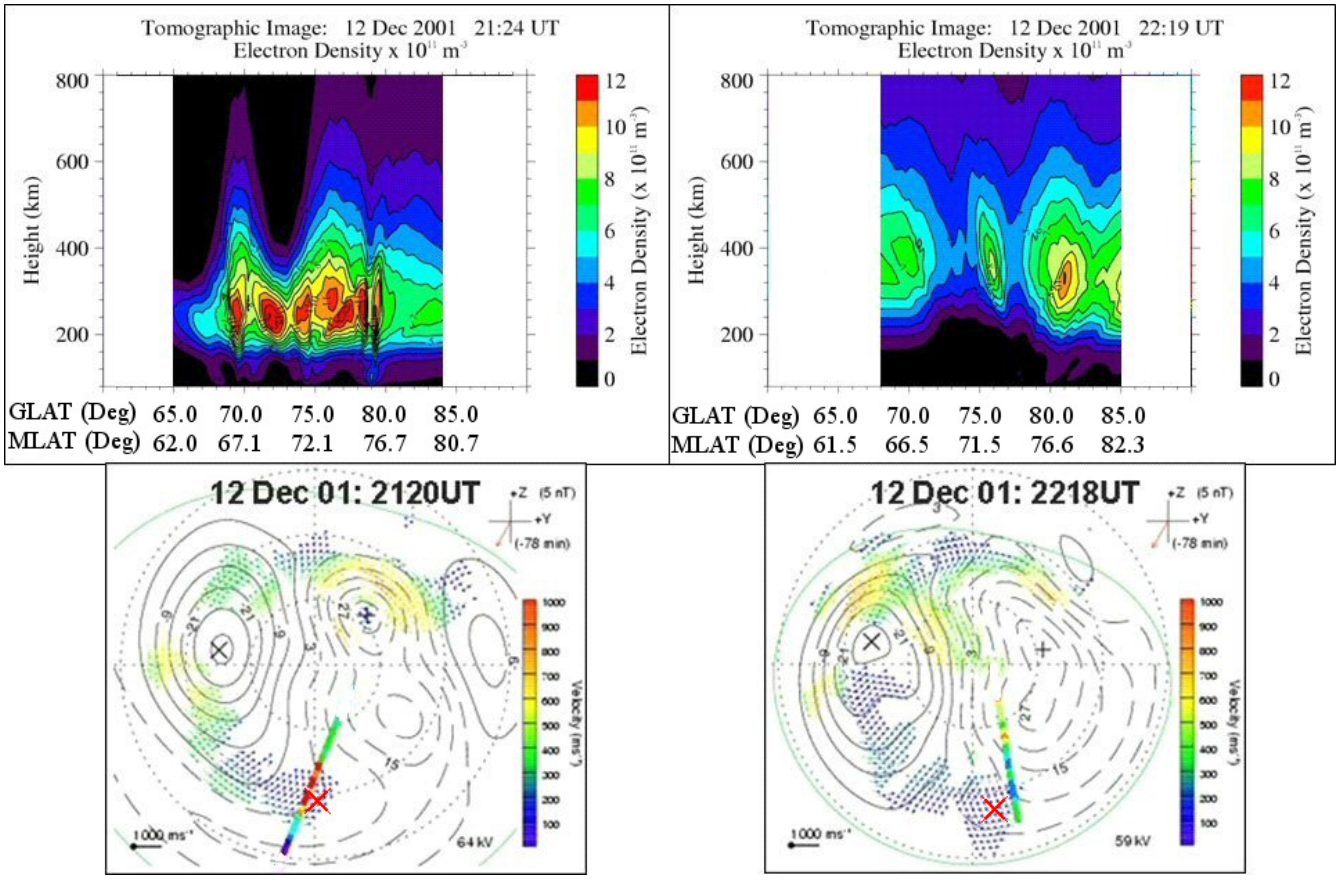

Fig. 5. Radiotomography reconstructions of electron densities for satellite passes that crossed a latitude of 75° N at 21:24 UT (top left panel) and 22:19 UT (top right panel), and corresponding SuperDARN electric potential patterns at 21:20 UT (bottom left panel) and 22:18 UT (bottom right panel). The multicoloured lines on the potential maps indicate the 350 km intersections of the respective satellite trajectories, with the colours representing the peak F-region electron densities of the tomography images. The red crosses represent the position of the 30 min running mean of the Spectral Width Boundary as inferred from the observations by beam 6 of the Hankasalmi SuperDARN radar at this time.

enhancements ruled out in situ precipitation as a source, and it was likely that the plasma had originated on the dayside and had been transported in the convective flow over the polar cap into the nightside. This interpretation was consistent with Bust and Crowley (2007) who applied a trajectory tracking technique to plasma density observations in this sector on 12 December 2001 and showed that the flux tubes were drawn from the high-latitude dayside ionosphere. By strict definition enhancements located within the polar cap are termed patches while those equatorward of the OCB are boundary blobs (Crowley, 1996). In the present study all of the density enhancements were attributed to transport of plasma from the dayside ionosphere and, in the main, occurred poleward of the OCB, although some were near the boundary. However, the distinction between patches and boundary blobs was not of significance for this study and for convenience both were referred to as patches. The influence of geomagnetic substorm activity on the spatial distribution of the structuring was of particular interest. This study complements the earlier work of Lorentzen et al. (2004), who used airglow as proxy for polar patches and revealed that the velocity of the patches as they flowed into the OCB was modulated by the phase of the substorm. The present study used direct observations of electron density by the ESR radar and radio tomography, rather than optical emission, inferred the motion of the OCB from electron temperature measurements and modulation in plasma drift from the SuperDARN radar network. Comparisons of the density structures with the high-latitude electric potential patterns were used to explain the modulation of the spatial distribution of polar patches by the substorm activity.

Signatures of the substorm activity during the evening of 12 December 2001 were identified by several instruments. Ground-based magnetometer observations of the horizontal magnetic field component provided direct evidence of two substorms separated by some two hours. The expansion and

contraction of the electric potential pattern on similar cycle times was evident in the SuperDARN observations, with the electric potential pattern being largest during substorm expansion and the early recovery phase and more contracted between the two substorms. This two-cycle pattern was also evident in the electron temperatures measured by the ESR radar. The sharp boundary between the regions of lower and higher electron temperatures was used as a proxy for the OCB. The poleward migration of elevated temperatures was a clear signature of the expansion of the auroral region to higher latitudes during the substorms. The 150 m s^{-1} SWB measured by the SuperDARN Hankasalmi radar also responded to the substorm activity, with the boundary moving rapidly poleward through some 2°–4° latitude at substorm expansion and early recovery. This was used to estimate the latitudinal movement of the OCB. While the two cycle pattern was evident there was no clear one-to-one relationship between the finer details of the variations due to additional changes in the SWB on timescales shorter than those of the substorm.

Two types of density enhancements were identified in the observations by the ESR radar in both azimuthal directions (Fig. 3). The first type was distinct polar patches. Such structures were observed from about 19:55 UT to 21:15 UT and also leading up to about 23:05 UT, with both intervals corresponding to substorm onset, expansion and recovery. Close inspection of these structures, in particular for the earlier time interval, showed the temporal separation of the features reducing with increasing time as the substorm subsided. The second density regime was defined by an enhancement that seemed to be continuous in the radar data. Of particular interest was the region between about 21:15 UT and 22:15 UT, which occurred in the interval between the two substorms. Close inspection revealed variation on a small temporal scale in the density level within this enhancement however, it was not possible to resolve regular individual features in the radar data. A second similar region was observed by the ESR leading up to midnight and comparison with the continuation of the magnetometer record into the following day showed that this also corresponded to a period in between substorms. However, this second region was not considered further in this study as it was at a time when the ESR radar was beginning to move out of the Harang discontinuity. The tomography images (Fig. 5) revealed the spatial structure of the plasma essentially co-located with the ESR measurements. The earlier tomography image at 21:24 UT monitored in between the two substorms was within the time that the ESR was observing the more continuous density enhancement, and showed a highly-structured ionosphere comprising structures in close proximity on scales of $\sim$2° latitude. This suggested that the continuous enhancement observed by the ESR was structured on small scales that were beyond the resolution of the operating mode of the radar. The later tomography pass at 22:19 UT was coincident with substorm expansion and showed individual density enhancements separated by some 5° latitude. The collective observations suggest that the patches crossed the OCB in both the premidnight and postmidnight sectors, consistent with the statistical study of Moen et al. (2007). It is likely that the patches observed in the postmidnight sector would form the poleward wall of the mid-latitude trough in the postmidnight sector as reported by Middleton et al. (2008).

The results clearly suggest that the density structuring of the nightside ionosphere was modulated by the substorm activity. Under the pertinent stable IMF conditions it was unlikely that the nightside structure was caused by modulations of the plasma high-latitude flow due to dayside magnetospheric reconnection. The time taken for plasma to cross the polar cap was estimated to be 2.5 h using the convection patterns inferred from the SuperDARN radars. When this delay was applied to the time of interest the convection pattern was observed to be highly stable on the dayside, extending to (70°$\pm$1°) MLAT with the boundary between the dawn and dusk cells located at (12$\pm$1) MLT. It is therefore highly unlikely that the source of the structuring was in the dayside ionosphere. In situ particle precipitation was also ruled out as the cause of the nightside plasma structure. Analysis of the ESR density structuring provided estimation of the repetition times between successive electron density maxima. For the first substorm the time intervals estimated from the top panel of Fig. 3 were 30, 17, 13 and 8 min respectively, whilst those between the patches in the third panel of the figure were 25, 13 and 13 min respectively. The larger interval corresponded to substorm expansion, with the spacing reducing as the recovery progressed. The interval between the density structures corresponding to the second substorm in the time interval leading up to 23:05 UT estimated from the top panel of Fig. 3 was 30 min. The ionospheric signatures of this substorm were not so pronounced as those for the first and the separations between the features observed in the second radar beam could not be estimated. All values obtained were within the patch repetition times of 5 to 30 min observed by Lorentzen et al. (2004), although there is evidence in the current study that the repetition time decreased during substorm recovery. The ESR velocity measurements show that the spatial separation of the patches during the substorm was between 2° and 4.5° latitude, with the separation decreasing as the substorm recovered. It is appreciated that there is much variability in the values of the measured parameters and the flow direction, nevertheless it is of note that these separations are broadly in-keeping with the patch spatial separations. Those observed in the 21:24 UT tomography reconstruction, which was in the interval between the substorms, were of some 2° latitude and those observed in the 22:19 UT tomographic image, which was close to the start of the second substorm, were of some 5° latitude.

The explanation of the modulation of the plasma structure by substorm activity is likely to be straight forward with the structuring not being caused directly by the substorm, but rather a consequence of the influence of the substorm on the

high-latitude convection pattern. Under conditions of storm expansion, the convective flow is expanded with the region poleward of the OCB being well within the rapid antisunward flow as it emerges from the polar cap. In between the substorms the convection pattern is contracted, with the region of interest lying closer to the divergence region of the Harang discontinuity, nearer the equatorward edge of the convection pattern. This in turn modulates the flow in the region poleward of the OCB, allowing the patches to move rapidly during substorm expansion, but with a reducing velocity as the substorm subsides. The plasma slows as the features move into the divergence region of the Harang discontinuity, with the patches effectively bunching into closer proximity. The poleward motion of the OCB during substorm expansion may also contribute to the effect, causing the region poleward of the OCB to be further upstream in the cross polar flow under the active conditions. However, it is unlikely that this plays a significant role in the observations presented here, with the OCB being generally equatorward of the patches observed by the ESR and the radio tomography throughout the period of interest.

4 Conclusions

Dayside ionisation, in the form of enhanced patches transported through the polar cap, plays an important role in the structure of the nightside ionospheric plasma. Observations of the patches in the vicinity of the nightside antisunward flow were made during a period of two successive geomagnetic substorms, which showed that the plasma structure poleward of the OCB depended on the phase of substorm activity. During substorm expansion and early recovery the patches were separated in latitude by some 5°, whereas in an interval between the substorm activity the separation was markedly reduced to about 2° latitude. The patch repetition interval was about 17–30 min during substorm expansion, but reduced during the recovery. These observations complement the earlier study of Lorentzen et al. (2004), by providing direct measurements of the electron density rather than by proxy of F-region airglow, with the repetition intervals being in good agreement.

The multi-instrument approach of this current study has enabled the interpretation of the plasma structuring during two substorms with the variation in patch repetition time and separation being attributed to expansion and contraction of the nightside high-latitude convection pattern. The region of interest, poleward of the OCB, was in the fast antisunward flow when the convection pattern was large during substorm expansion, but in slower flow near the divergence region of the Harang discontinuity when the pattern was contracted. In the faster flow the patches were separated by some 5° latitude, but within the slower drift in the region of divergence the ionosphere was structured on smaller horizontal scales of some 2° latitude.

Acknowledgements. Financial support for the project was provided by the UK Science and Technology Facilities Council under grant PP/E001157/1, the Norwegian Research Council and Air Force Office of Scientific Research, Air Force Material Command, USAF, under grant number FA8655-06-1-3060. The assistance of the University of Tromsø and the Norwegian Polar Research Institute in the tomographic measurements is gratefully acknowledged. The Tromsø magnetogram was provided by Tromsø Geophysical Observatory, University of Tromsø. The SuperDARN radar facility is funded by the National Research Programs of Australia, Canada, Finland, Japan, South Africa, Sweden, UK and USA. The electric potential map data was provided by the University of Leicester and the discussion of the data with Mark Lester is gratefully acknowledged. EISCAT is an international facility supported by the national science councils of China, Finland, France, Germany, Japan, Norway, Sweden and the United Kingdom. The IMF data was provided by N. Ness and obtained from the CDAWeb. AGW acknowledges receipt of a STFC postgraduate studentship.

Topical Editor M. Pinnock thanks D. Lorentzen and another anonymous referee for their help in evaluating this paper.

References

Bowline, M. D., Sojka, J. J., and Schunk, R. W.: Relationship of theoretical patch climatology to polar cap patch observations, Radio Sci., 31, 635–644, 1996.

Buchau, J., Reinisch, B. W., Weber, E. J., and Moore, J. G.: Structure and dynamics of the winter polar cap F-region, Radio Sci., 18, 995–1010, 1983.

Buchau, J., Weber, E. J., Anderson, D. N., Carlson Jr., H. C., Moore, J. G., Reinisch, B. W., and Livingston, R. C.: Ionospheric structures in the polar cap: their origin in relation to 250-MHz scintillation, Radio Sci., 20, 325–338, 1985.

Bust G. S. and Crowley, G.: Tracking of polar cap ionospheric patches using data assimilation, J. Geophys. Res., 112, A05307, doi:10.1029/2005JA011597, 2007.

Carlson, H. C.: Role of neutral atmospheric dynamics in cusp density and ionospheric patch formation, Geophys. Res. Lett., 34, L13101, doi:10.1029/2007GL029316, 2007.

Carlson, H. C., Oksavik, K., Moen, J., van Eyken, A. P., and Guio, P.: ESR mapping of polar-cap patches in the dark cusp, Geophys. Res. Lett., 29, 1386, doi:10.1029/2001GL014087, 2002.

Carlson, H. C., Moen, J., Oksavik, K., Nielsen, C. P., McCrea, I. W., Pedersen, T. R., and Gallop, P.: Direct observations of injection events of subauroral plasma into the polar cap, Geophys. Res. Lett., 33, L05103, doi:10.1029/2005GL025230, 2006.

Chisham, G., Freeman, M. P., and Sotirelis, T.: A statistical comparison of SuperDARN spectral width boundaries and DMSP particle precipitation boundaries in the nightside ionosphere, Geophys. Res. Lett., 31, L02804, doi:10.1029/2003GL019074, 2004.

Chisham, G., Lester, M., Milan, S. E., Freeman, M. P., Bristow, W. A., Grocott, A., MacWilliams, K. A., Ruohoniemi, J. M., Yeoman, T. K., Dyson, P., Greenwald, R. A., Kikuchi, T., Pinnock, M., Rash, J., Sato, N., Sofko, G., Villain, J.-P., and Walker, A. D. M.: A decade of the Super Dual Auroral Radar Network (SuperDARN): Scientific achievements, new techniques and future directions, Surv. Geophys., 28, 33–109, doi:10.1007/s10712-007-9017-8, 2007.

Crowley, G.: Critical review of ionospheric patches and blobs, URSI Review of Radio Science 1993–1996, edited by: Stone, W. R., 619–648, 1996.

Foster, J. C.: Ionospheric signatures of magnetospheric convection, J. Geophys. Res., 89, 855–865, 1984.

Greenwald, R. A., Baker, K. B., Dudeney, J. R., Pinnock, M., Jones, T. B., Thomas, E. C., Villain, J.-P., Cerisier, J.-C., Senior, C., Hanuise, C., Hunsucker, R. D., Sofko, G., Koehler, J., Nielsen, E., Pellinen, R., Walker, A. D. M., Sato, N., and Yamagishi, H.: Darn/Superdarn: A global view of the dynamics of high-latitude convection, Space Sci. Rev., 71, 761–796, 1995.

Lockwood, M. and Carlson Jr., H. C.: Production of polar cap electron density patches by transient magnetopause reconnection, Geophys. Res. Lett., 19, 1731–1734, 1992.

Lorentzen, D. A., Shumilov, N., and Moen, J.: Drifting airglow patches in relation to tail reconnection, Geophys. Res. Lett., 31, L02806, doi:10.1029/2003GL017785, 2004.

McEwen, D. J. and Harris, D. P.: Occurrence patterns of F layer patches over north magnetic pole, Radio Sci., 31, 619–628, 1996.

Middleton, H. R., Pryse, S. E., Wood, A. G., and Balthazor, R. L.: The role of the tongue-of-ionisation in the formation of the poleward wall of the main trough in the European post-midnight sector, J. Geophys. Res., 113(A2), A02306, doi:10.1029/2007JA012631, 2008.

Moen, J., Carlson, H. C., Oksavik, K., Nielsen, C. P., Pryse, S. E., Middleton, H. R., McCrea, I. W., and Gallop, P.: EISCAT observations of plasma patches at sub-auroral cusp latitudes, Ann. Geophys., 24, 2363–2374, 2006, http://www.ann-geophys.net/24/2363/2006/.

Moen J., Gulbrandsen, N., Lorentzen, D. A., and Carlson, H. C.: On the MLT distribution of F region polar cap patches at night, Geophys. Res. Lett., 34, L14113, doi:10.1029/2007GL029632, 2007.

Moen, J., Lockwood, M., Oksavik, K., Carlson, H. C., Denig, W. F., van Eyken, A. P., and McCrea, I. W.: The dynamics and relationships of precipitation, temperature and convection boundaries in the dayside auroral ionosphere, Ann. Geophys., 22, 1973–1987, 2004, http://www.ann-geophys.net/22/1973/2004/.

Moen, J., Qiu, X. C., Carlson, H. C., Fujii, R., and McCrea, I. W.: On the diurnal variability in F2-region plasma density above the EISCAT Svalbard radar, Ann. Geophys., 26, 2427–2433, 2008, http://www.ann-geophys.net/26/2427/2008/.

Østgaard, N., Moen, J., Mende, S. B., Frey, H. U., Immel, T. J., Gallop, P., Oksavik, K., and Fujimoto, M.: Estimates of magnetotail reconnection rate based on IMAGE FUV and EISCAT measurements, Ann. Geophys., 23, 123–134, 2005, http://www.ann-geophys.net/23/123/2005/.

Pedersen, T. R., Fejer, B. G., Doe, R. A., and Weber, E. J.: An incoherent scatter radar technique for determining two-dimensional horizontal ionization structure in polar cap F region patches, J. Geophys. Res., 105, 10637–10655, 2000.

Pryse, S. E.: Radio tomography: A new experimental technique, Surv. Geophys., 24, 1–38, 2003.

Pryse, S. E., Sims, R. W., Moen, J., Kersley, L., Lorentzen, D., and Denig, W. F.: Evidence for solar-production as a source of polar-cap plasma, Ann. Geophys., 22, 1093–1102, 2004, http://www.ann-geophys.net/22/1093/2004/.

Pryse, S. E., Wood, A. G., Middleton, H. R., McCrea, I. W., and Lester, M.: Reconfiguration of polar-cap plasma in the magnetic midnight sector, Ann. Geophys., 24, 2201–2208, 2006, http://www.ann-geophys.net/24/2201/2006/.

Pryse, S. E., Whittick, E. L., Aylward, A. D., Middleton, H. R., Brown, D. S., Lester, M., and Secan, J. A.: Modelling the tongue-of-ionisation using CTIP with SuperDARN electric potential input: verification by radiotomography, Ann. Geophys., 27, 1139–1152, 2009, http://www.ann-geophys.net/27/1139/2009/.

Rino, C. L., Livingston, R. C., Tsunoda, R. T., Robinson, R. M., Vickrey, J. F., Senior, C., Cousins, M. D., Owen, J., and Klobuchar, J. A.: Recent studies of the structure and morphology of auroral-zone F-region irregularities, Radio Sci., 18, 1167–1180, 1983.

Robinson, R. M., Tsunoda, R. T., Vickrey, J. F., and Guerin, L.: Sources of F region ionisation enhancements in the nighttime auroral zone, J. Geophys. Res., 90, 7533–7546, 1985.

Rodger, A. S., Pinnock, M., Dudeney, J. R., Baker, K. B., and Greenwald, R. A.: A new mechanism for polar patch formation, J. Geophys. Res., 99, 6425–6436, 1994.

Ruohoniemi, J. M. and Baker, K. B.: Large-scale imaging of high-latitude convection with Super Dual Auroral radar Network HF radar observations, J. Geophys. Res., 103, 20797–20806, 1998.

Schunk, R. W., Zhu, L., and Sojka, J. J.: Ionospheric response to travelling ionospheric vortices, Geophys. Res. Lett., 21, 1759–1763, 1994.

Sims, R. W., Pryse, S. E., and Denig, W. F.: Spatial structure of summertime ionospheric plasma near magnetic noon, Ann. Geophys., 23, 25–37, 2005, http://www.ann-geophys.net/23/25/2005/.

Smith, A. M., Pryse, S. E., and Kersley, L.: Polar patches observed by ESR and their possible origin in the cusp region, Ann. Geophys., 18, 1043–1053, 2000, http://www.ann-geophys.net/18/1043/2000/.

Sojka, J. J., Bowline, M. D., Schunk, R. W., Decker, D. T., Valladares, C. E., Sheehan, R., Anderson, D. N., and Heelis, R. A.: Modelling polar-cap F-region patches using time-varying convection, Geophys. Res. Lett., 20, 1783–1786, 1993.

Valladares, C. E., Basu, S., Buchau, J., and Friis-Christensen, E.: Experimental evidence for the formation and entry of patches into the polar cap, Radio Sci., 29, 167–194, 1994.

Walker, I. K., Moen, J., Kersley, L., and Lorentzen, D. A.: On the possible role of cusp/cleft precipitation in the formation of polar-cap patches, Ann. Geophys., 17, 1298–1305, 1999, http://www.ann-geophys.net/17/1298/1999/.

Weber, E. J., Buchau, J., Moore, J. G., Sharber, J. R., Livingston, R. C., Winningham, J. D., and Reinisch, B. W.: F-layer ionization patches in the polar cap, J. Geophys. Res., 89, 1683–1694, 1984.

Weber, E. J., Klobuchar, J. A., Buchau, J., Carlson Jr., H. C., Livingston, R. C., de la Beaujadiere, O., McCready, M., Moore J. G. and Bishop, G. J.: Polar cap F layer patches: Structure and dynamics, J. Geophys. Res., 91, 12121–12129, 1986.

Wood, A. G., Pryse, S. E., Middleton, H. R., and Howells, V. S. C.: Multi-instrument observations of nightside plasma patches under conditions of IMF B_z positive, Ann. Geophys., 26, 2203–2216, 2008, http://www.ann-geophys.net/26/2203/2008/.